A Method for Planning Safe Trajectories in Image-Guided Keyhole Neurosurgery

Reuben R. Shamir[1], Idit Tamir[2], Elad Dabool[1], Leo Joskowicz[1], and Yigal Shoshan[2]

[1] School of Engineering and Computer Science, The Hebrew University, Jerusalem, Israel
[2] Dept. of Neurosurgery, Hebrew University Hadassah Medical Center, Jerusalem, Israel
rubke@cs.huji.ac.il

Abstract. We present a new preoperative planning method for reducing the risk associated with insertion of straight tools in image-guided keyhole neurosurgery. The method quantifies the risks of multiple candidate trajectories and presents them on the outer head surface to assist the neurosurgeon in selecting the safest path. The surgeon can then define and/or revise the trajectory, add a new one using interactive 3D visualization, and obtain a quantitative risk measures. The trajectory risk is evaluated based on the tool placement uncertainty, on the proximity of critical brain structures, and on a predefined table of quantitative geometric risk measures. Our results on five targets show a significant reduction in trajectory risk and a shortening of the preoperative planning time as compared to the current routine method.

1 Introduction

Many image-guided keyhole neurosurgery procedures require the precise targeting of tumors and anatomical structures with a surgical tool inside the brain based on pre-operative CT/MRI images. A misplacement of the surgical tool from the planned trajectory may result in non-diagnostic tissue samples and/or severe neurological complications [1-2]. Consequently, it is desired to select a trajectory that is at a safe distance from critical structures such as blood vessels and motor and functional areas.

In current practice, trajectory planning is performed manually and may be sub-optimal, as it requires the surgeon to mentally reconstruct complex 3D brain structures and their relations based on 2D cross-sections of the patient pre-operative CT/MRI head images. The treatment risk and implications evaluation is thus a complex and time-consuming task. While volume visualization and spatial segmentation of critical brain structures are sometimes used to help the neurosurgeon with spatial perception and planning, the insertion trajectory is currently determined manually. Furthermore, it does not include any quantitative measures or trajectory-specific visualization of nearby critical structures. The resulting trajectory is thus surgeon-dependent and may not be optimal.

Several studies have proposed methods to better assess and reduce risk in image guided neurosurgery [3-10]. Some of them are aimed at tasks that are significantly different from insertion of a straight surgical tool. They include methods for identifying targets and trajectories in Deep Brain Stimulation (DBS) based on a statistical atlas [5], for optimizing a path within intracranial blood vessels [7], for path optimization

T. Jiang et al. (Eds.): MICCAI 2010, Part III, LNCS 6363, pp. 457–464, 2010.
© Springer-Verlag Berlin Heidelberg 2010

for optimal tumor evacuation [8], and for planning of non-straight trajectories with non-interactive, time-consuming optimization methods [4].

In recent work, Lee et al. [9] propose a method to fuses patient MRI head images with a registered atlas to support the manual selection of a trajectory with a visualization of the 3D atlas structures. Its main disadvantage is that the trajectory is selected manually without any quantitative information regarding nearby critical structures. Vaillant et al. [10] computes the risk of a candidate trajectory with a weighted sum and based on the trajectory intersected intracranial structures and their associated importance. The weakness of this method is that it does not consider the distance of a structure from the trajectory; thus, the damage that can be caused by surgical tool misplacement is not incorporated in the function. Tirelli et al. [3] assign each candidate trajectory with a risk value that is based on a weighted sum; the drawbacks are that no risk visualization or quantitative feedback is provided. Brunenberg et al. [6] show that computing the risk with a weighted sum can be misleading and suggest computing the maximum risk value instead. The Euclidean distance of the trajectory from critical brain structures is used to compute the risk of each voxel. Their method outputs tens to hundreds of trajectories associated with distances above a predefined threshold. Although the method significantly reduces the number of possible trajectories, it still leaves a considerable amount of manual work without quantitative feedback. Moreover, none of the studies evaluated their contribution to the actual reduction of the risk.

We present a novel preoperative straight trajectory planning method for image-guided keyhole neurosurgery. Our method quantifies the risks of multiple candidate trajectories and presents them on the outer head surface to assist the neurosurgeon in selecting the safest path. For visualization, we color-code all the trajectories according to their associated risk level and present them all at once on the relevant parts of the outer head surface. The surgeon can then select and revise the trajectory, and add or edit trajectories with visual 3D feedback and updated risk information. Our method incorporates interactive 3D visualization of critical structures and of surgical tool placement uncertainty. The computed trajectory is presented to the physician along with a 'risk card' that includes quantitative risk measures such as the length of the trajectory and distance between the trajectory and closest blood vessels. We observe that reporting only the maximum risk value may be partial and incomplete and compute both: the maximum and the summation of risks along trajectory. Moreover, we conduct a clinical comparative study on MRI head images to rate our method vs. routine planning on five targets.

2 Method Overview

We propose the following eight-step preoperative planning workflow for image guided keyhole neurosurgery (Fig. 1). Initially, (1) the neurosurgeon selects the target location on the CT/MRI preoperative image. Then, (2) the head outer surface is computed automatically and the neurosurgeon defines (3) the surface region on which the entry point should be located. Afterwards, (4, 5) the anatomical structures of interest for the surgery, e.g. blood vessels and ventricles, are segmented and assigned a risk value based on the potential damage of penetrating them with a surgical tool (this is done once for all patients). The input segmentations and the assigned risk values are

automatically combined into a single volume (6), called the *risk volume*, in which voxel intensity is associated with a value representing the level of damage that may be caused by a surgical tool passing through it. A trajectory risk value is then computed (7) for each trajectory automatically and the candidate trajectories risks are color-coded and superimposed on the defined entry points surface to form risk maps (Fig. 2). Finally, (8) the neurosurgeon interactively selects and refines a trajectory with visual and quantitative feedback (Figs. 2 and 3).

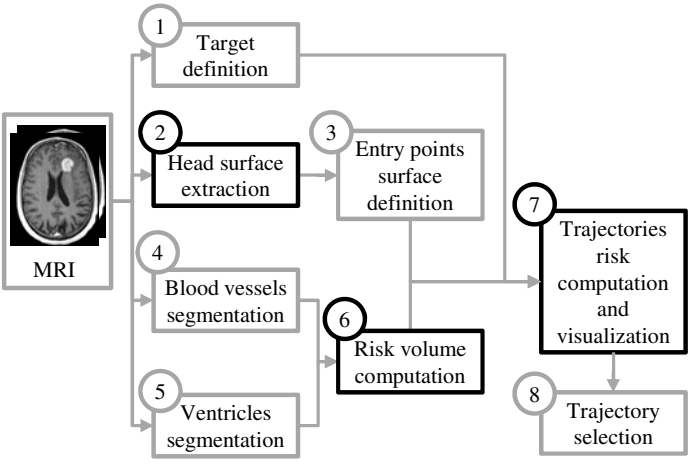

Fig. 1. Preoperative planning workflow for image guided keyhole neurosurgery

We define a risk card as a summary of geometrical parameters regarding critical structures and planned trajectories. The risk card provides the neurosurgeon with valuable information regarding the assessment of an intervention's risk and enables the direct quantitative comparison between candidate trajectories. The relevant risk parameters were identified by a senior neurosurgeon. They include measures for assessing trajectory's risk such as trajectory length, and distances of trajectory, target and entry to closest blood vessels and ventricles.

We use graphical illustrations to assist the surgeon in understanding the geometrical meaning of the measures. For example, when the neurosurgeon points with the cursor on the risk card trajectory length column, it is illustrated graphically (Fig. 3). Trajectories can be added and modified based on the 3D visualization of their localization uncertainty and predefined critical structures. The visualization of tool localization uncertainty eases the identification of cases where a planned line trajectory does not cross a critical structure, including the placement uncertainty, and indicates the possible damage to critical structures.

We describe next our method for the computation of the risk volume, the trajectory risk, and the visualization of multiple trajectories risks.

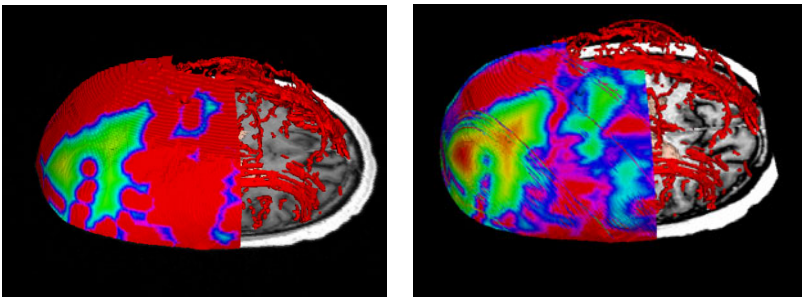

(a) Maximum (b) Summation

Fig. 2. Risk maps of candidate trajectories with two computation methods: (a) maximum, and; (b) summation of voxels in the risk volume that are intersected by the trajectory. Red zones are associated with high-risk trajectories. Green and yellow zones indicate safer entry points.

2.1 Computation of Risk Volume

Each voxel in the risk volume is assigned with the estimated cost incurred by penetrating the corresponding region with a surgical tool. The risk volume is generated based on two key guidelines: 1) the risk value is directly related to the estimated consequences and severity of the damage to the corresponding brain tissue or organ, severe complications and high morbidity regions are assigned with a higher risk values than tissues with minor and reversible complications, and; 2) voxels near critical structures are assigned with high risk values to reflect the intrinsic localization error of the procedure, be it freehand, frame-based stereotaxy, or with an image-guided surgery system. Therefore, voxels that are closer to a critical structure are associated with a higher risk value than those that reside further from them.

The input is a set of critical structures for which insertion of a surgical tool is forbidden or undesired, $S = \{S_1, S_2, \ldots, S_p\}$, and their associated risk values $R = \{r_1, r_2, \ldots, r_p\}$. The structure S_i is a segmented image. The risk value r_i is a non-negative scalar. We define each voxel in the risk volume as:

$$riskVolume\left(\overline{x}\right) = max\left\{\frac{r_k}{dist\left(\overline{x}, S_k\right) + \alpha}\right\}_k \tag{1}$$

where $\overline{x}$ is the voxel center location and α is a non-negative scaling constant. Eq. 1 assigns to each voxel the maximal expected risk computed with the above cost function and with respect to the input structures and risk values. For $\alpha = 1$ and distance $dist\left(\overline{x}, S_k\right) = 0$ (e.g. voxel is located on the structure) the voxel value is the same as the input risk value r_k. It decreases as the voxel is further from the structure.

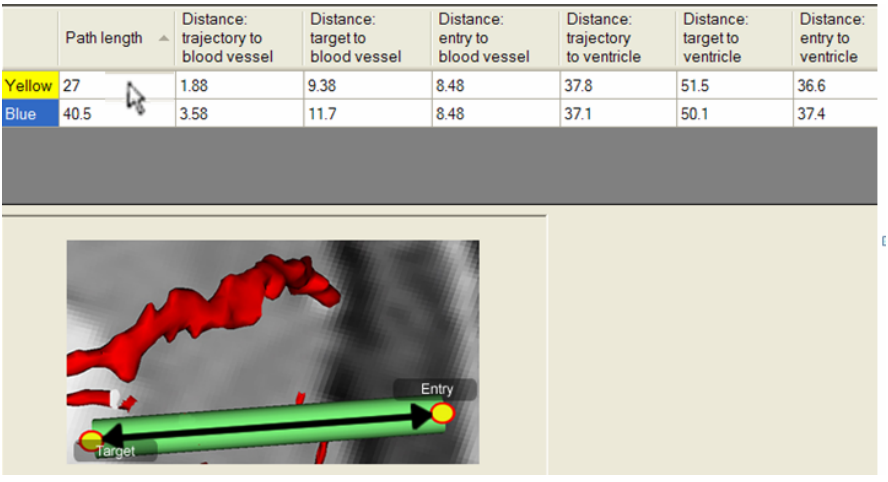

Fig. 3. Trajectory risk card showing seven parameters (all values in mm) and 3D illustration image of the "path length" risk parameter

In practice, we expect the neurosurgeon to define only a handful of risk levels, i.e., risk values $R = \{r_1, r_2, \ldots, r_p\}$ are selected from a small group of numbers $r_i \in \{0,1,2,...,c\}$. In cases where two or more structures are associated with the same risk level, the voxel risk value is associated with the closest structure distance (Eq. 1). This allows computing one distance map for multiple structures that are associated with same risk level. With this approach, few distance maps can cover a large set of segmented structures.

2.2 Trajectory Risk Computation and Visualization

We assign to a given trajectory two risk values: 1) the maximal value, and 2) the sum of voxels in the risk volume that are intersected by the trajectory. The input is a target location, *t*, a set of candidate entry points $\{e_1, e_2, \ldots, e_n\}$, and the risk volume *riskVolume*. Each target and candidate entry point pair defines a trajectory $tr_i = [e_i; t]$. The maximal trajectory risk is:

$$risk_{max}\left(tr_i, riskVolume\right) = max\left\{riskVolume\left(\bar{x}\right)\right\}_{\bar{x} \cap tr_i \neq \varnothing} \quad (2)$$

Note that this definition of trajectory risk does not incorporate some important risk factors such as path length and thus provides only partial information regarding the trajectory risks. For example, this definition cannot differentiate between cases where many blood vessels surround the trajectory and those where only one blood vessel is

within its proximity. Therefore, it is also desired to compute the sum of the voxels risk values along the trajectory. This measure better reflects path length, and incorporates all risks occur along the path. Note that this measure is also incomplete and should be considered with the maximal risk [6].

$$risk_{sum}\left(tr_i, riskVolume\right) = \sum_{\bar{x} \cap tr_i \neq \varnothing} riskVolume\left(\bar{x}\right) \tag{3}$$

To assist the neurosurgeon in selecting the safest paths, we propose a visualization of the relevant candidate entry-points zones on the outer head surface. Each candidate entry point on the relevant outer head surface zone is colored with respect to the risk value that was computed on its trajectory (Fig. 2). The user can change the risk computation method (Eqs. 2 or 3), the color-map, and can change the position and orientation of the 3D surface.

3 Experimental Results

We compared our method to the current routine manual approach for trajectory planning on five targets selected at various locations on four clinical MRI head images. The images are 512×512×122 voxels^3 with voxel size of 0.47×0.47×1.0 mm^3. For each target, a specialist neurosurgeon selected two trajectories: one with the conventional method based on the axial, sagittal, and coronal 2D views of the original MRI images, and the second trajectory was selected with our method. The planning protocol was as in Fig 1. A target was initially defined on the MRI image. Then, the outer surface of the head was automatically segmented and extracted [12], and sampled with ~40K points. For each target, the user defined surface areas on the outer head surface from which the entry point can be chosen. Each candidate entry point defines a candidate trajectory with the predefined target. The blood vessels and ventricles were semi-automatically segmented and their surfaces were reconstructed. Distance maps are computed with the method of Danielsson et al. [11]. The blood vessels were associated with a risk level of $r_1 = 255$ and the ventricles were associated with a risk level of $r_2 = 100$. The risk volume was computed using Eq. 1 with r_1 and r_2 as above and $\alpha = 1$.

For each possible trajectory, the risk volume voxels that were intersected by the trajectory were identified, and the trajectory risk was computed using Eq. 2 and 3. Next, the trajectories risks were color-coded and superimposed on the relevant part of the head surface. The neurosurgeon then interactively selected an entry point. The corresponding risk card was automatically computed and a 3D visualization of the localization uncertainty and blood vessels was generated and displayed for further refinement. The method was implemented with the Visualization ToolKit (VTK) [13] and the Insight segmentation and registration ToolKit (ITK) [14] and was integrated as a set of modules in Slicer [15] on a standard PC running Windows XP OS.

Table 1. Comparison of the proposed and routine methods. Target codes are: **LF** – Left and(delet) Frontal, **LFTI** – Left Fronto-Tempo-Insular, **RPO** – Right Parieto-Occipital, **LFP** – Left Frontal-Periventricular, and **MP** - Medial Perichiasmatic and anterior to the Midbrain.

Target number	Target location	Method	Trajectory length(mm)	Distance: Trajectory to Blood Ves-sels(mm)	Distance: Trajectory to Ventricles (mm)	Time (min)
1	LF	Routine	35.2	5.15	9.99	-
		Proposed	31.6	9.39	9.52	-
2	LFTI	Routine	27.0	1.88	37.8	19
		Proposed	40.5	3.58	37.1	6
3	RPO	Routine	25.6	12.0	26.3	9
		Proposed	29.1	12.0	26.3	9
4	LFP	Routine	56.2	7.16	12.0	9
		Proposed	57.8	7.99	13.1	6
5	MP	Routine	94.4	0.0	2.74	6
		Proposed	96.3	1.0	4.9	10
Average		Routine	47.7	5.2	17.8	10.8
		Proposed	51.0	6.8	18.1	7.7

Table 1 summarizes the results. The mean trajectory planning time using the routine method was 10.8 min (range 6-19 min) compared to a mean of 7.7 min (range 6-10 min) using our method. Using the routine method, the mean distance of a planned trajectory to closest Blood Vessel (BV) and closest ventricle are 5.2mm (range 0.0-12.0 mm) and 17.8 mm (range 2.7-37.8 mm), respectively. Our method yielded mean distances of 6.8 mm (range 1.0-12.0 mm) from a blood vessel and 18.1mm (range 4.9-37.1 mm) from closest ventricle. The mean trajectory length with the routine method was 47.7mm (range 25.6-94.4 mm) compared to 51.0mm (range 29.1-96.3 mm) using our method.

4 Discussion

In cases 1, 2, and 5 our method resulted in significantly larger distances of up-to 4mm between trajectories and their closest blood vessel or ventricle. In cases 3 and 4, no significant difference was observed. The reason for the lack of improvement in case 3 is that the target point is located near the cranial surface where it was easier for the neurosurgeon to evaluate the risks and define a trajectory with the routine method. In case 4, the target location was the closest point along the trajectory to nearest blood vessel and the ventricle, and therefore no improvement was recorded.

The neurosurgeon that evaluated our method reports that it increased the control and confidence levels, and improved the risk assessment. The colorization of outer head surface facilitated the entry point selection. The 3D visualization of blood vessels greatly helped in understanding their complex structure and their spatial relations with respect to the planned trajectory. The risk card assisted in the trajectory selection.

5 Conclusions

We have presented a novel method to enhance the conventional trajectory planning method by a visualization of trajectories risks and by providing quantitative risk information and interactive 3D visualization of localization uncertainty and structures associated with a high risk for better assessment of the possible risks in image guided keyhole neurosurgery. Our experimental results suggest that our method produces safer trajectories in which a misplacement of a surgical tool is less likely to damage a critical structure.

Acknowledgements

This work was supported by FP7 ERC ROBOCAST Grant No. 21590.

References

1. Shamir, R.R., Joskowicz, L., Spektor, S., Shoshan, Y.: Localization and registration accuracy in image guided neurosurgery: a clinical study. Int. J. Comput. Assist. Radiol. Surg. 4(1), 45–52 (2009)
2. Mascott, C.R.: In vivo accuracy of image guidance performed using optical tracking and optimized registration. J. Neurosurgery 105(4), 561–567 (2006)
3. Tirelli, P., de Momi, E., Borghese, N.A., Ferrigno, G.: An intelligent atlas-based planning system for keyhole neurosurgery. In: Computer Assisted Radiology and Surgery (CARS 2009) supplemental, pp. S85–S86 (2009)
4. Popovic, A., Trovato, K.: Path planning for reducing tissue damage in minimally invasive brain access. In: Computer Assisted Radiology and Surgery (CARS 2009) supplemental, pp. S132–S133 (2009)
5. Guo, T., Parrent, A.G., Peters, T.M.: Automatic target and trajectory identification for deep brain stimulation (DBS) procedures. In: Ayache, N., Ourselin, S., Maeder, A. (eds.) MICCAI 2007, Part I. LNCS, vol. 4791, pp. 483–490. Springer, Heidelberg (2007)
6. Brunenberg, E.J., Vilanova, A., Visser-Vandewalle, V., Temel, Y., Ackermans, L., Platel, B., et al.: Automatic trajectory planning for deep brain stimulation: a feasibility study. In: Ayache, N., Ourselin, S., Maeder, A. (eds.) MICCAI 2007, Part I. LNCS, vol. 4791, pp. 584–592. Springer, Heidelberg (2007)
7. Fujii, T., Emoto, H., Sugou, N., Mito, T., Shibata, I.: Neuropath planner–automatic path searching for neurosurgery. In: Computer Assisted Radiology and Surgery (CARS), pp. 587–596 (2003)
8. Bourbakis, N.G., Awad, M.: A 3-D visualization method for image-guided brain surgery. IEEE Trans. Syst. Man Cybern., Part B: Cybern. 33(5), 766–781 (2003)
9. Lee, J.D., Huang, C.H., Lee, S.T.: Improving stereotactic surgery using 3-D reconstruction. IEEE Eng. Med. Biol. Mag. 21(6), 109–116 (2002)
10. Vaillant, M., Davatzikos, C., Taylor, R.H., Bryan, R.N.: A path-planning algorithm for image-guided neurosurgery. In: First Joint Conference Computer Vision, Virtual Reality and Robotics in Med. and Med. Robotics and Comp. Assisted Surgery, pp. 467–476 (1997)
11. Danielsson, P.E.: Euclidean distance mapping. Computer Vision, Graphics, and Image Processing, 227–248 (1980)
12. Joskowicz, L., Shamir, R., Freiman, M., Shoham, M., Zehavi, E., Umansky, F., et al.: Image-guided system with miniature robot for precise positioning and targeting in keyhole neurosurgery. Comput. Aided Surg. 11(4), 181–193 (2006)
13. The Visualization Toolkit (VTK), `http://www.vtk.org/`
14. The Insight Segmentation and Registration Toolkit (ITK), `http://www.itk.org/`
15. 3D Slicer, `http://www.slicer.org/`